Self-assembled gold nanoparticles on functionalized gold(111) studied by scanning tunneling microscopy

PENG, Zhang-Quan(彭章泉) WANG, Er-Kang*(汪尔康)

Laboratory of Electroanalytical Chemistry, Changchun Institute of Applied Chemistry, Chinese Academy of Sciences, Changchun, Jilin 130022, China

Nanogold colloidal solutions are prepared by the reduction of $HAuClO_4$ with sodium citrate and sodium borohydride. 4-Aminothiophenol (ATP) self-assembled monolayers (SAMs) are formed on gold(111) surface, on which gold nanoparticles are immobilized and a sub-monolayer of the particles appears. This sub-monolayer of gold nanoparticles is characterized with scanning tunneling microscopy (STM), and a dual energy barrier tunneling model is proposed to explain the imageability of the gold nanoparticles by STM. This model can also be used to construct multiple energy barrier structure on solid/liquid interface and to evaluate the electron transport ability of some organic monolayers with the aid of electrochemical method.

Keywords Gold nanoparticle, SAM, STM, energy barrier

Introduction

Metal nanoparticles have become a subject of intense interest in material and physical chemistry.[1] Their unique physical properties caused by the quantum-size and surface effects[2] give rise to a wide variety of potential applications such as sensor, nanoelectronic devices and catalysts. But nanoparticles have a tendency to agglomerate because of their large surface/volume ratio. So, the first thing is to immobilize and characterize the nanoparticles in order to gain their special properties. As the development of molecular self-assembly technique,[3] it has demonstrated that highly dispersed gold colloidal particles can also self-assemble on the surface of self-assembled monolayers (SAMs) with certain tail groups, such as $-NH_2$, -SH moieties,[4] which opens a wide path to confine nanoparticles for further investigation. The commonly used techniques[5] to characterize the particles are scanning electron microscopy (SEM) and transmission electron microscopy (TEM) whose probes are electron beams, and the result gained by those techniques is creditable for the wave length of the electron beams being much smaller than the dimension of the particles under investigation. Scanning tunneling microscopy is a surface analytical technique with the highest resolution to atomic scale.[6] But application of STM to investigate metal particles self-assembled on functionalized organic monolayers is seldom for the reasons that the particles do not directly contact with the conductive substrate but are spaced out by an insulating organic monolayer, and the convolution between STM tip and particles. It seems that this organic monolayer has no negative effect on the imaging of nanoparticles as demonstrated by some previous work[7] just like that non-conductive biomolecules can also be imaged by STM. So what happens in the system composed of STM tip, metal particles, organic monolayer and conductive substrate during the process of imaging is ambiguous and a controversial topic. In this work 4-aminothiophenol was self-assembled on Au(111) surface, then gold colloidal nanoparticles self-assembled on the functionalized SAMs, leading to arrays of gold/organic molecules/gold structures on the substrate. The attached gold nanoparticles were characterized by STM, and the whole fabrication process was shown in Fig. 1. The imageability of the particles by STM showed that there must be electron tunneling between particles and

* Received February 15, 2000; accepted April 25, 2000.
Project (No. 29975028) supported by the National Natural Science Foundation of China.
Corresponding author's e-mail: *ekwang@mail.jlu.edu.cn*

substrate besides between STM tip and particles, so a dual barrier model was proposed to explain the STM imaging process according to our experimental results. This model can also be used to construct multiple energy barrier structure on solid/liquid interface and to evaluate the electron transport ability of some organic monolayers with the aid of electrochemical method.

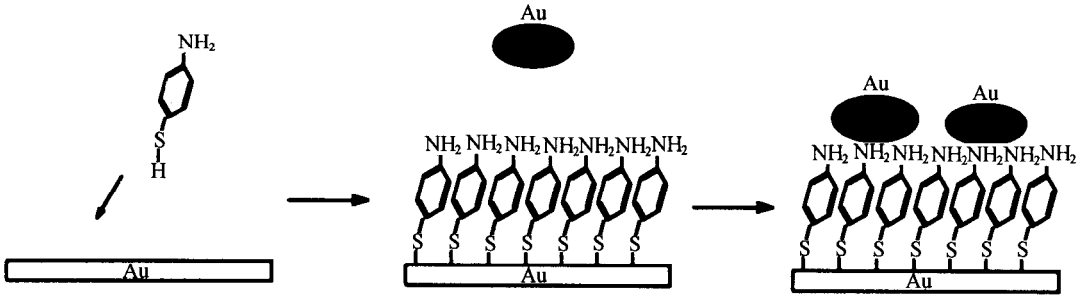

Fig. 1 Schematic diagram for colloidal Au nanoparticals assembling on 4-aminothiophenol SAMs modified gold(111) substrate.

Experimental

Preparation of nanogold colloidal solutions

According to method from Natan group[5] with a slight modification, 0.8 mL of 1.0% sodium citrate and 0.3 mL of 0.075% sodium borohydride were blended into 100 mL of aqueous solutions. The mixture was then rapidly added into 100 mL of solutions of 2.0% $HAuCl_4$ with furious stirring. After further stirring for 2 h, the color of the resultant solution turned from weak yellow to rosy colour. Finally the gold colloidal solutions were kept in refrigerator at 4℃ for further use.

Monolayer self-assembly and gold nanoparticle self-assembly

4-Aminothiophenol monolayers for STM examination were prepared by immersion of the gold(111) substrate sample in a ca. 0.001 M 4-aminothiophenol solution in ethanol for 48 h. The resultant substrate with functionalized surface was dipped into the gold colloidal solutions for 2 h, then taken out and thoroughly rinsed by ethanol, finally dried in nitrogen. Polycrystalline gold was also used as a substrate to form SAMs for electrochemical examination by the similar way as that of gold (111) substrate.

Electrochemical measurements

Electrochemical measurements were performed using a three-electrode cell comprising the gold working electrode, a platinum flag counter electrode, and an Ag/AgCl reference electrode. For cyclic voltammetry (CV) measurements, a CHI 500 A. C. Impedance Analyzer (CH Instruments, Inc.) was employed under control of a computer.

Scanning tunneling microscopy (STM)

STM imaging was performed at room temperature in air using a Nanoscope IIIa microscope (Digital Instruments, Inc.). The samples were scanned in the constant current mode using a homemade tungsten tip.

Results and discussion

Electron tunneling through two energy barriers

Electron tunneling through barriers whose energy is greater than that of the tunneling electron is a common phenomenon in nanoworld. When electron tunnels through one barrier, the value of tunneling probability is very small, and it will rapidly decrease as the barrier width increases. When electron tunnels through two barriers, it is intuitive that the electron will encounter more difficulties and that the tunneling probability will be even smaller. But this is not always the truth. Here we will simply discuss that the electron tunnels through two rectangular barriers and give the necessary and qualitative result. When electron is confined in metal component in this model, we treat it as free electron.

Fig. 2 is the scheme of electron tunneling through

two barriers. In range of I to V, the electron wave functions must meet the time-independent Schrodinger equation: $\boldsymbol{H}\Psi = E\Psi$, and the common solution is:

$$\Psi_i = a_i\exp(ik_ix) + b_i\exp(-ik_ix),\ k_i = 2m(E - U_i)^{1/2}/H,\ i = 1,2,3,4,5;\ H = h/2\pi \quad (1)$$

where $\boldsymbol{H}$ is the Hamilton operator, E is the total energy of electron, Ψ_i is the wave function, a_i and b_i are the pre-exponential factors, m is the mass of electron, U_i is the potential funtion of the electron and h is the Plank constant. In order to simplify the expressions, we define $k_2 = i\kappa_2$, $k_4 = i\kappa_4$.

Barriers I and IV are the energy forbidden zone in classical mechanics, but quantum mechanics deems that electron can tunnel although the total electron energy is less than the height of the energy barrier. According to the natural properties of wave functions shown below:

$$\Psi_i(x_i) = \Psi_{i+1}(x_i),\ \Psi'_i(x_i) = \Psi'_{i+1}(x_i),\ i = 1,2,3,4 \quad (2)$$

we can ultimately obtain the rate of tunneling (T) from I to IV,

$$\begin{aligned} T &= [(\boldsymbol{H}k_5/m)\mid a_5\mid^2]/[(\boldsymbol{H}k_1/m)\mid a_1\mid^2] \\ &= (2^8k_1\kappa_2{}^2k_3{}^2\kappa_4{}^2k_5)/[(k_1^2 + \kappa_2^2)(\kappa_2^2 + k_3^2)(k_3^2 + \kappa_4^2)(\kappa_4^2 + k_5^2)\mid K\mid^2] \end{aligned} \quad (3)$$

$$\begin{aligned} K = {} & 2i\exp(\kappa_2d_2 + \kappa_4d_4)[\sin(-k_3d_3 + \theta_3 + \theta_4)\exp i(\theta_2 + \theta_5)] \\ & + 2i\exp(\kappa_2d_2 - \kappa_4d_4)[\sin(k_3d_3 - \theta_3 + \theta_4)\exp i(\theta_2 - \theta_5)] \\ & + 2i\exp(-\kappa_2d_2 + \kappa_4d_4)[\sin(k_3d_3 + \theta_3 - \theta_4)\exp i(-\theta_2 + \theta_5)] \\ & + 2i\exp(-\kappa_2d_2 - \kappa_4d_4)[\sin(k_3d_3 - \theta_3 - \theta_4)\exp i(-\theta_2 - \theta_5)], \end{aligned} \quad (4)$$

$$\theta_2 = \tan^{-1}(\kappa_2/k_1),\ \theta_3 = \tan^{-1}(\kappa_2/k_3),\ \theta_4 = \tan^{-1}(\kappa_4/k_3),\ \theta_5 = \tan^{-1}(\kappa_4/k_5)$$
If we assume that $\kappa_2d_2 = \kappa_4d_4$, $k_3d_3 = \theta_3 + \theta_4 + 2n\pi$ (n is an integer) (5)

so $K = 2i[\sin2\theta_4\exp i(\theta_2 - \theta_5) + \sin2\theta_3\exp i(-\theta_2 + \theta_5)]$, and the exponential relationship between the T and the energy barrier width will no longer fit. The value of T is considerably enlarged and not related with the position of the barriers too.

When we further assume that $k_1 = \kappa_2 = k_3 = \kappa_4 = k_5$ and $k_3d_3 = (n + 1/2)\pi$, we will find that the value of T is 1. It means that under these rigid conditions, dual energy barriers have not any block effect on the electron tunneling through them.[8] This phenomenon is the so-called electron resonance tunneling in quantum mechanics.

Summary, electron can tunnel through dual energy barriers, and the tunneling rate under certain conditions is considerably large. This dual energy barrier model can be used to explain the STM imaging of gold nanoparticles spaced out by organic monolayers on substrate. Theoretically, as long as the value of the x_i can meet the conditions of Eq. (4) or (5), the satisfying tunneling probability will be achieved. While under real conditions, the formal T will be smaller slightly than that under the ideal conditions for the deformation of the energy barrier shape induced by the interaction of the adjacent barriers.

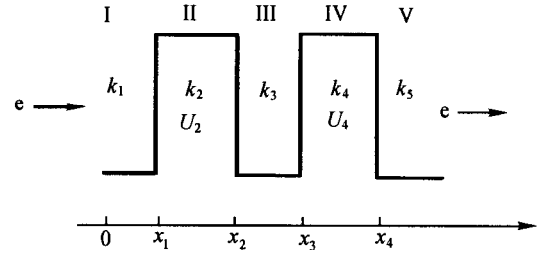

Fig. 2 Scheme of dual rectangular barriers for electron tunneling [x_i (i = 1—4) represents the position of the barriers, respectively].

Electron tunneling through two barriers between STM *tip and substrate*

Fig. 3 is a scheme for electron tunneling between STM tip and gold substrate. In this system there are two energy barriers, one is the gap between STM tip and the anchored gold nanoparticles which is common metal/metal tunneling junction, and the other is the organic monolayer whose electron block behavior has been examined by cyclic voltammetry (CV) experiments taking $Fe(CN)_6^{3-/4-}$ as a probe. From the enlarged peak separation (ΔE_p) and depressed current compared with those at bare gold electrode as shown in Fig. 4, we think that the organic monolayer has block effect on the interfacial charge transfer and treat it as an energy barrier in the process of STM imaging of gold particles. When a sample is scanned in constant current mode under certain bias voltage, there is electron tunneling through the organic monolayer at the same time when electron tunneling through the gap between the STM tip and the gold nanoparticles. And we can not deny the emergence of some interesting situations such as $\kappa_2 d_2 = \kappa_4 d_4$, $k_3 d_3 = \theta_3 + \theta_4 + 2n\pi$ in the process of imaging. Considering the function of the feed-back control system in STM equipment, the gold nanoparticles spaced out by electron block monolayer can always be imaged just by adjusting the gap width between the STM tip and the gold nanoparticles automatically when the bias voltage and setpoint current are set constant. And the imaging of gold nanoparticles by STM gives the experimental proof undoubtedly that there are tunneling currents between the STM tip and the substrate. The STM image of ATP self-assembled monolayers with the attached gold particles is shown in Fig. 5. The real size of the nanoparticles is less than the result obtained by STM for the convolution between STM tip and particles, which also results in a little distortion of the nanoparticles.

This double energy barrier model can also be employed to evaluate the conducting or block properties of the self-assembled monolayers between the gold substrate and the attached gold nanoparticles by electrochemical method. It has been well known that some common redox probes such as $Fe(CN)_6^{3-/4-}$ can give a fast and reversible response by using electroanalytical method such as cyclic voltammetry and a.c. impedance at bare gold electrode surface, but not at the surface of self-assembled monolayer. So, we can attach some amount of gold nanoparticles on the surface of SAMs as arrays of microelectrodes linked by the affinity moieties of the SAMs. From the different electrochemical response, we can infer the electron transport ability of the SAM clusters between the electrode matrix and the nanoparticles. Applying this concept we have examined the electron transport abilities of some dithiols, and satisfying experimental results have been gained.

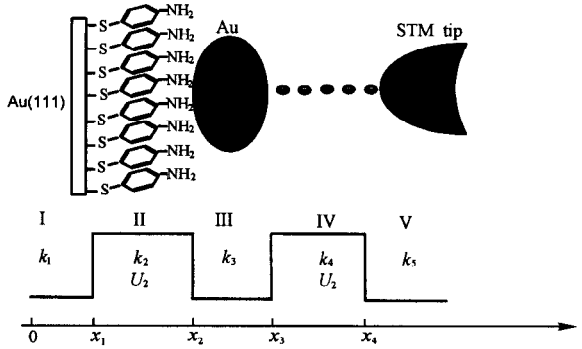

Fig. 3 A simple dual barrier model while gold nanoparticles are imaged by STM [x_i (i = 1—4) represents the relative position of the barriers from Au(111) substrate to the STM tip].

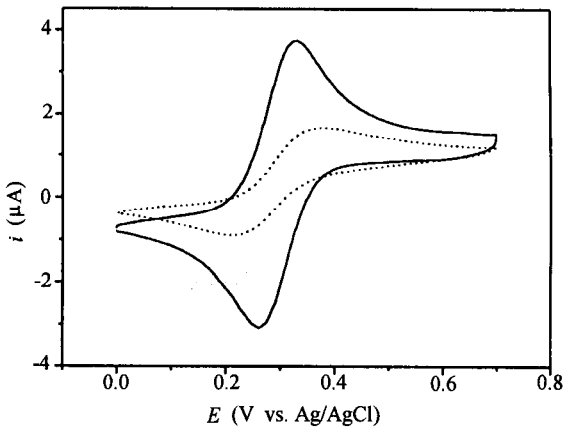

Fig. 4 Cyclic voltammetric curves obtained for the gold electrode in 0.005 M $K_4Fe(CN)_6$ before (solid line) and after (dot line) the ATP modification, scan rate was 0.05 V/s, supporting electrolyte was 0.05 M NaH_2PO_4 + 0.05 M Na_2HPO_4.

Conclusions

A dual energy barrier model was proposed to explain the imageability of the gold nanoparticles spaced

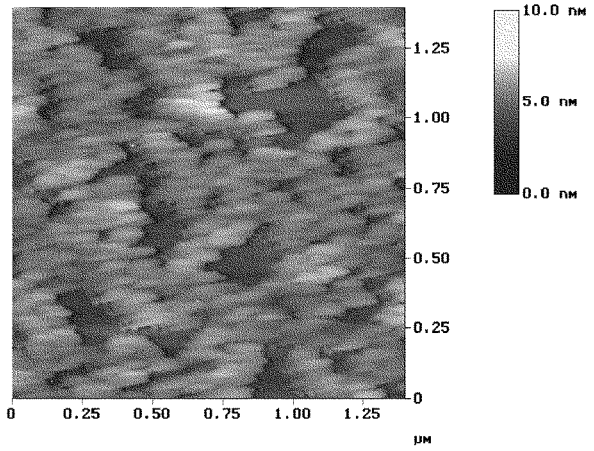

Fig. 5 STM image of gold particles taken in air on ATP SAMs supported by Au(111), bias voltage was 0.12 V and tunneling current was 1 nA.

out by organic monolayer with scanning tunneling microscopy. This model can also be constructed at solid/liquid interfacial by molecular self-assembly technique and nanogold preparation technique, and be used to evaluate the electron transport abilities of the concerned SAMs.

References

1. Brown, L.O.; Hutchison, J.E., *J. Am. Chem. Soc.*, **121**, 882(1999).
2. Hermann, W.A., *Angew. Chem. Int. Ed. Engl.*, **25**, 56(1986).
3. Delamarche, E.; Michel, B.; Biebuyck, H.A., *Adv. Mater.*, **8**, 719(1996).
4. Zhu, T.; Zhang, X.; Wang, J.; Fu, X.; Liu Z., *Thin Solid Films*, **327-329**, 595(1998).
5. Grabar, K.C.; Brown, K.R.; Keating, C.K.; Stranick, S.J.; Tang, S.; Natan, M.J., *Anal. Chem.*, **69**, 471 (1997).
6. Poirier, G.E., *Chem. Rev.*, **97**, 1117(1997).
7. Kind, H.; Bittner, A.M.; Canella, O.; Kern, K., *J. Phys. Chem. B*, **102**, 7582(1998).
8. Lindsay, S.M.; Sankey, S.F.; Li, Y.; Herbst, C.; Rupprecht, A., *J. Phys. Chem.*, **94**, 4655(1990).

(E200002027 JIANG, X.H.; LING, J.)